Sliding-mode observer for speed-sensorless induction motor drives

S. Xepapas, A. Kaletsanos, F. Xepapas and S. Manias

Abstract: A sliding-mode observer for the speed-sensorless direct torque vector control of induction motors is proposed. The observer estimates the motor speed, the rotor flux, the angular position of the rotor flux and the motor torque from measured terminal voltages and currents. The use of the nonlinear sliding-mode technique provides very good performance for both low- and high-speed motor operation and robustness in motor losses and load variations. The proposed observer does not uses a PI controller and complicated observer gains and that establishes an easy setup for any type of motor. Also, the convergence of the proposed observer is examined using the Lyapunov theory. Experimental results using a TMS320F240 digital signal processor are presented for low–speed operation (5 Hz), full speed operation (50 Hz), and forward to reverse operation. Finally, the proposed observer is compared with other recently reported model-reference adaptive system techniques.

1 Introduction

In the past, several methods for speed-sensorless control of induction machines have been proposed [1–4].

Magnetic-Salience-Based methods [5, 6] are very promising for standstill and low-speed operation. Their main disadvantage is the need for high precision voltage and current measurements. Also, these methods require a proper machine design.

Model-Reference Adaptive Systems (MRASs) [7–10] are methods that have a good performance over a large speed range. Their disadvantage is the large influence of parameter deviation at low-speed and standstill operation. Also, the use of PI controllers with complicated gains creates difficulties in their implementation using a digital signal processor (DSP) or microcontrollers.

The extended Kalman filter [11, 12] has for several years been used as the most appropriate solution for speed-sensorless drives. Unfortunately, this stochastic observer has some inherent disadvantages, such as the influence of the noise characteristic, the computational burden and the absence of design and tuning criteria.

The current harmonic spectral estimation method [13] estimates the rotor speed from current harmonics, which arise from rotor mechanical and magnetic saliencies, that are independent of motor parameters and with a magnitude that is independent of the source frequency. This method seems to have a very good performance at low speed, even at 1 Hz, but needs a complicated hardware/software setup for measuring and filtering the currents.

IEE Proceedings online no. 20030882

doi: 10.1049/ip-cta:20030882

Paper first received 8th August 2002 and in revised form 24th July 2003

The authors are with Power Electronics Research Laboratory, Department of Electrical and Computer Engineering, National Technical University of Athens, Athens, Greece

Artificial intelligence methods [14] that use artificial intelligence techniques such as fuzzy logic and neural networks are very promising candidates to be robust to parameter deviation and measurement noise but they need long development times and an expertise in several artificial intelligence procedures.

From the above methods the most promising candidate to be robust, accurate with a fast convergence and a small computational time, seems to be those that are based in a MRAS. Most of these conventional methods use PI controllers with complicated gain calculations. These gains have the best performance for a specific load. Also, a knowledge of the motor - load inertia and friction is important. The performance of the PI controller is directly dependent on these parameters; especially in the case of a variable load where the PI controllers can't have the same behaviour over the full speed range. Also, the implementation of very small gains in a fixed point DSP is very difficult and a high accuracy is needed. As a result, the use of a PI controller ensures the best performance of the system for specific operational conditions i.e. for constant load or for low- or high-speed operation.

Lately, an adaptive sliding-mode observer for speed-sensorless control has been proposed [15]. This observer seems to have a very good performance over the full speed range because of the sliding-mode technique, however, the calculation of several observer gains is needed. Also, the use of very small gain values leads to serious problems during the implementation.

A sliding-mode observer is now presented for speed-sensorless motor drive systems. The proposed observer estimates the motor speed, the rotor flux, the angular position of the rotor flux and the motor torque in a robust and efficiency manner. Also, only one observer gain is needed.

The use of the non-linear sliding-mode technique has the following advantages:

(i) Good and stable performance over the full frequency range from as low as 1 Hz until the nominal operation at 50 Hz.

(ii) Robustness to the parameter sensitivity over the full speed range.
(iii) Ease of implementation without complicated gains.

The proposed observer is part of a sliding-mode fuzzy logic control technique for sensorless induction motor drive systems [16]. Its behaviour and robustness has been tested using simulation and experimental results.

2 Motor and proposed observer models

The induction motor can be described analytically by the following state equations in the stationary reference frame d,q. [3]:

$$\frac{d\lambda_{dr}}{dt} = \lambda'_{dr} = -n\lambda_{dr} - \omega_r\lambda_{qr} + nL_m i_{ds} \tag{1}$$

$$\frac{d\lambda_{qr}}{dt} = \lambda'_{qr} = -n\lambda_{qr} + \omega_r\lambda_{dr} + nL_m i_{qs} \tag{2}$$

$$\frac{di_{ds}}{dt} = i'_{ds} = \beta n\lambda_{dr} + \beta\omega_r\lambda_{qr} - \gamma i_{ds} + \frac{1}{\sigma L_s}u_{ds} \tag{3}$$

$$\frac{di_{qs}}{dt} = i'_{qs} = \beta n\lambda_{qr} - \beta\omega_r\lambda_{dr} - \gamma i_{qs} + \frac{1}{\sigma L_s}u_{qs} \tag{4}$$

$$T_e = \left(\frac{3P}{4}\right) \times \frac{L_m}{L_r} \times \left(i_{qs}\lambda_{dr} - i_{ds}\lambda_{qr}\right) = \text{const} \times \left(i_{qs}\lambda_{dr} - i_{ds}\lambda_{qr}\right) \tag{5}$$

$$\frac{d\omega_r}{dt} = \frac{P}{2} \times \frac{1}{J} \times (T_e - T_L) - T_{\omega_r} \tag{6}$$

The meaning of the above symbols and the definition of the constant values are given in Appendix A.

For sensorless control it is necessary to make a simultaneous observation of the rotor flux and rotor speed. The proposed observer belongs to the category of closed-loop systems and its design [17] is the following:

$$\frac{d\hat{\lambda}_{dr}}{dt} = \hat{\lambda}'_{dr} = -n\hat{\lambda}_{dr} - \hat{\omega}_r\hat{\lambda}_{qr} + nL_m i_{ds} \tag{7}$$

$$\frac{d\hat{\lambda}_{qr}}{dt} = \hat{\lambda}'_{qr} = -n\hat{\lambda}_{qr} + \hat{\omega}_r\hat{\lambda}_{dr} + nL_m i_{qs} \tag{8}$$

$$\frac{d\hat{i}_{ds}}{dt} = \hat{i}'_{ds} = \beta n\hat{\lambda}_{dr} + \beta\hat{\omega}_r\hat{\lambda}_{qr} - \gamma\hat{i}_{ds} + \frac{1}{\sigma L_s}u_{ds} \tag{9}$$

$$\frac{d\hat{i}_{qs}}{dt} = \hat{i}'_{qs} = \beta n\hat{\lambda}_{qr} - \beta\hat{\omega}_r\hat{\lambda}_{dr} - \gamma\hat{i}_{qs} + \frac{1}{\sigma L_s}u_{qs} \tag{10}$$

where $\hat{i}_{ds}$ and $\hat{i}_{qs}$ are the estimated stator current components, $\hat{\lambda}_{dr}$ and $\hat{\lambda}_{qr}$ are the estimated rotor flux components and $\hat{\omega}_r$ is the estimated value of the motor speed. Using the following definitions:

$$\bar{i}_{ds} = \hat{i}_{ds} - i_{ds},\ \bar{i}_{qs} = \hat{i}_{qs} - i_{qs},\ \bar{\omega}_r = \hat{\omega}_r - \omega_r$$

$$\bar{\lambda}_{dr} = \hat{\lambda}_{dr} - \lambda_{dr},\ \bar{\lambda}_{qr} = \hat{\lambda}_{qr} - \lambda_{qr}$$

that expresses the mismatch between estimated and real components, a new system can be developed as follows:

$$\bar{i}'_{ds} = -\gamma\bar{i}_{ds} + \beta n\bar{\lambda}_{dr} + \beta\omega_r\bar{\lambda}_{qr} + \beta\bar{\omega}_r\hat{\lambda}_{qr} \tag{11}$$

$$\bar{i}'_{qs} = -\gamma\bar{i}_{qs} + \beta n\bar{\lambda}_{qr} - \beta\omega_r\bar{\lambda}_{dr} - \beta\bar{\omega}_r\hat{\lambda}_{dr} \tag{12}$$

$$\bar{\lambda}'_{dr} = -n\bar{\lambda}_{dr} - \bar{\omega}_r\hat{\lambda}_{qr} - \omega_r\bar{\lambda}_{qr} \tag{13}$$

$$\bar{\lambda}'_{qr} = -n\bar{\lambda}_{qr} + \bar{\omega}_r\hat{\lambda}_{dr} + \omega_r\bar{\lambda}_{dr} \tag{14}$$

3 Stability analysis of the proposed observer

3.1 Current mismatch stability

Let us define the following positive Lyapunov function:

$$I = \frac{1}{2}\left(\bar{i}_{ds}^2 + \bar{i}_{qs}^2\right) \geq 0$$

Its derivative $I' = \bar{i}'_{ds}\bar{i}_{ds} + \bar{i}'_{qs}\bar{i}_{qs}$ after substitution from (11) and (12) can be written as follows:

$$I' = -2\gamma I - \beta\omega_r(\hat{s}_n - s_n) - \beta\bar{\omega}_r\hat{s}_n + \beta n s_c \tag{15}$$

where

$$\hat{s}_n = \bar{i}_{qs}\hat{\lambda}_{dr} - \bar{i}_{ds}\hat{\lambda}_{qr}$$
$$s_n = \bar{i}_{qs}\lambda_{dr} - \bar{i}_{ds}\lambda_{qr}$$
$$s_c = \bar{i}_{ds}\bar{\lambda}_{dr} + \bar{i}_{qs}\bar{\lambda}_{qr}$$

The current mismatch dynamics are stable if the conditions $I' < 0$ and $I \geq 0$ are true. The sufficient condition $I' < 0$ can be written as follows:

$$\omega_r(\hat{s}_n - s_n) + \bar{\omega}_r\hat{s}_n > -\frac{2\gamma}{\beta}I + n s_c \tag{16}$$

If the following equation is selected:

$$\hat{\omega}_r = K\text{sgn}(\hat{s}_n) \tag{17}$$

then is sufficient to state:

$$K|\hat{s}_n| > \omega_r|s_n| + \delta \geq \omega_r s_n + \delta \tag{18}$$

where

$$\delta = -\frac{2\gamma}{\beta}I + n s_c$$

If K is big enough, (18) holds and estimated current values $\hat{i}_{ds}$ and $\hat{i}_{qs}$ will converge to the real ones $i_{ds}, i_{qs}(\bar{i}_{ds} \to 0, \bar{i}_{ds} \to 0, \hat{s}_n \to 0)$.

3.2 Rotor Flux mismatch stability

When $\hat{\omega}_r = K\text{sgn}(\hat{s}_n)$, in the state-space model the curve $\hat{s}_n = 0$ is attractive for current mismatch dynamics. According to sliding-mode theory [18] under the discontinuous control $\hat{\omega}_r = K\text{sgn}(\hat{s}_n)$ the equivalent motion can be described by the set of equations $\hat{s}_n = 0, \hat{s}'_n = 0$. This leads to the following expression:

$$\hat{s}'_n = \beta n(\bar{\lambda}_{qr}\hat{\lambda}_{dr} - \bar{\lambda}_{dr}\hat{\lambda}_{qr}) - \beta\hat{\omega}_r(\hat{\lambda}_{dr}^2 + \hat{\lambda}_{qr}^2) + \beta\omega_r(\lambda_{dr}\hat{\lambda}_{dr} + \lambda_{qr}\hat{\lambda}_{qr}) = 0$$

or equivalently

$$\hat{\omega}_r = \hat{\omega}_r^{eq} = \omega_r \frac{(\lambda_{dr}\hat{\lambda}_{dr} + \lambda_{qr}\hat{\lambda}_{qr})}{(\hat{\lambda}_{dr}^2 + \hat{\lambda}_{qr}^2)} + n\frac{(\bar{\lambda}_{qr}\hat{\lambda}_{dr} - \bar{\lambda}_{dr}\hat{\lambda}_{qr})}{(\hat{\lambda}_{dr}^2 + \hat{\lambda}_{qr}^2)} \quad (19)$$

Substituting the equivalent speed value $\hat{\omega}_r^{eq}$ into (13) and (14), the following system of equations exist:

$$\begin{aligned}\bar{\lambda}'_{dr} &= \frac{-n\hat{\lambda}_{dr}^2 + \omega_r\hat{\lambda}_{dr}\hat{\lambda}_{qr}}{\left(\hat{\lambda}_{dr}^2 + \hat{\lambda}_{qr}^2\right)}\bar{\lambda}_{dr} + \frac{-\omega_r\hat{\lambda}_{dr}^2 - n\hat{\lambda}_{dr}\hat{\lambda}_{qr}}{\left(\hat{\lambda}_{dr}^2 + \hat{\lambda}_{qr}^2\right)}\bar{\lambda}_{qr} \\ \bar{\lambda}'_{qr} &= \frac{\omega_r\hat{\lambda}_{qr}^2 - n\hat{\lambda}_{dr}\hat{\lambda}_{qr}}{\left(\hat{\lambda}_{dr}^2 + \hat{\lambda}_{qr}^2\right)}\bar{\lambda}_{dr} + \frac{-n\hat{\lambda}_{qr}^2 - \omega_r\hat{\lambda}_{dr}\hat{\lambda}_{qr}}{\left(\hat{\lambda}_{dr}^2 + \hat{\lambda}_{qr}^2\right)}\bar{\lambda}_{qr}\end{aligned} \quad (20)$$

The roots of the characteristic polynomial of the above system are the following:

$$\rho_1 + \rho_2 = -n < 0 \quad \rho_1 = -n \quad \text{or} \quad \rho_1\rho_2 = 0 \quad \rho_2 = 0$$

Therefore, under feedback $\bar{\omega}_r = K\text{sgn}(\hat{s}_n)$, the proposed observer system is forced to slide on $\hat{s}_n = 0$ with equivalent value $\hat{\omega}_r = \hat{\omega}_r^{eq}$ and the system of (20) is neutrally stable ($\bar{\lambda}'_{dr} \to 0$, $\bar{\lambda}'_{qr} \to 0$, $\bar{\lambda}_{dr} = c_d$, $\bar{\lambda}_{qr} = c_q$ where c_d and c_q are constants). At steady state, (13) and (14) can be written as follows:

$$-nc_d - \omega_r c_q = \bar{\omega}_r\hat{\lambda}_{qr} \quad (21)$$

$$\omega_r c_d - nc_q = -\bar{\omega}_r\hat{\lambda}_{dr} \quad (22)$$

Because $\hat{\lambda}_{dr} = f_d(t)$ and $\hat{\lambda}_{qr} = f_q(t)$, the only solution for the above system of equations is $c_d = c_q = 0$ and $\bar{\omega}_r = 0$, which means that $\bar{\lambda}_{dr} = 0$, $\bar{\lambda}_{qr} = 0$ and $\hat{\omega}_r = \hat{\omega}_r^{eq}$.

In order to ensure the convergence of the proposed observer the control variable $\hat{\omega}_r = K\text{sgn}(\hat{s}_n)$ must be calculated as follows:

$$\hat{\omega}_r = \begin{cases} +K \text{ for } \hat{s}_n > 0 \\ -K \text{ for } \hat{s}_n < 0 \end{cases} \text{ where } K \geq \omega_{max} \quad (23)$$

Using (23) as feedback to the proposed observer, which is defined by (7)–(10), the convergence of the rotor flux and torque is fast and robust with the parameter variation using only one gain. In order to calculate the motor speed $\hat{\omega}_r^{eq} = \omega_r$, a low-pass filter must be used. Figure 1 shows the block diagram of the proposed observer.

The reason that the proposed observer exhibits a good performance is because the feedback is using the sliding-mode technique, resulting in the instant calculation of the rotor flux, the rotor flux angular velocity and the motor torque. The equivalent motor speed, $\hat{\omega}_r^{eq}$, is passed through a digital low-pass filter.

The above analysis proved that the observer gain K must be equal to or greater than ω_{max}. One matter that must be analysed is how large can the gain K become. Theoretical analysis and experiments lead to the following results:

(i) Increasing the gain K means that the ripple of $\hat{\omega}_r^{eq}$ is bigger. This leads to the conclusion that the digital low-pass filter needs to have a very low cutoff frequency. This is a disadvantage because the low-pass filter inserts a time delay.

(ii) Increasing the gain K means that the calculation of the rotor flux and motor torque is faster. Actually the proposed observer forces the system to converge to the correct value of the rotor flux. That convergence is instant when the gain K is very big, and in fact is theoretically infinite.

Therefore, the gain K is a critical constant of the proposed observer and can be chosen according to the application. Also, in the case of variable speed operation the gain K can also be variable. The system can automatically adjust the gain K in association with $\hat{\omega}_r^{eq}$. With a variable gain K the performance of the system is good and stable over the full speed range and the ripple of the equivalent motor speed is small in any case.

4 Experimental results

4.1 Experimental setup

The proposed sensorless observer has been tested in order to verify its behaviour and robustness using the experimental setup, that is shown in Fig. 2.

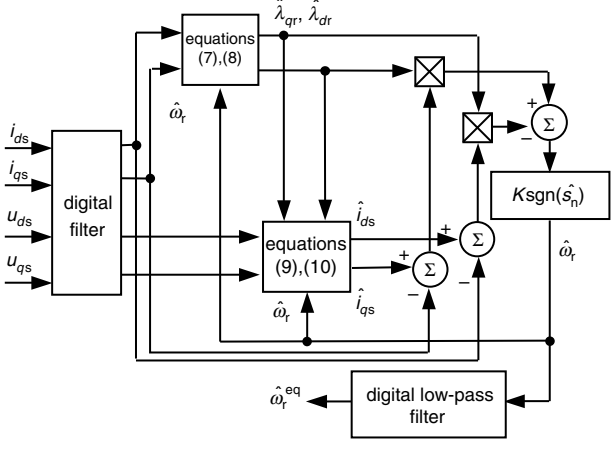

Fig. 1 *Block diagram of the proposed observer*

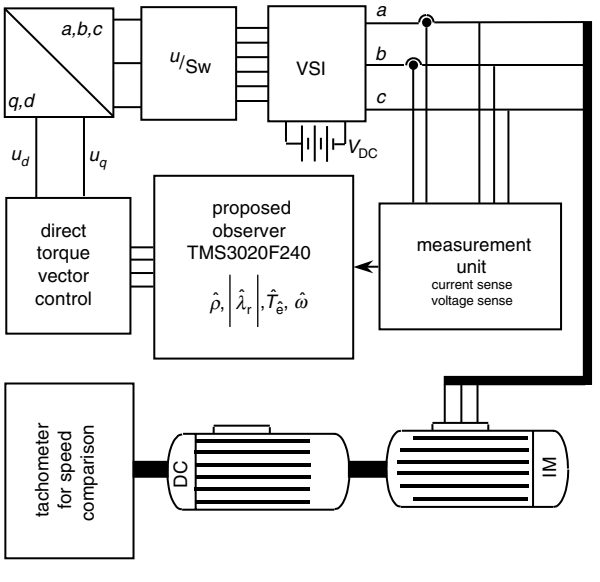

Fig. 2 *Block diagram of the experimental setup*

The setup consists of a 2.2 kW voltage source inverter controlled by a microprocessor (Intel 80C196), an induction motor, a DC motor for load, a measurement unit and for the implementation of the proposed observer a fixed point DSP (TMS320F240). The proposed observer that is implemented in the DSP, using a 40 kHz clock, consists of the following main routines:

Measurement routine: Every 10 kHz two phase-to-phase voltages and two line currents are measured using the onboard analog-to-digital converter. The conversion time per two analog signals is 6.6 μs.

Filter routine: In order to minimise the noise of the measured signals a digital FIR filter, (Bohman, type window) with ten terms has been used. The response of the filter was tested using the application 'fdatool' (filter design analysis tool) from Matlab. The transfer function of the digital filter is given in appendix B.

Transformation routine: With this routine the transformation from a, b, c to the stationery reference frame d,q takes place.

Equation routine: This routine solves the differential equations of the proposed observer using the fourth-order Runge-Kutta method (see Appendix C).

Sliding-mode routine: This routine implements the proposed sliding-mode technique with an observer gain $K = 314\,rad/s$ in order to estimate the motor speed. It also estimates all the necessary values for the direct torque vector control [16], $\hat{\rho}$, $|\hat{\lambda}_r|$, $\hat{T}_e$ ($\hat{\rho}$ is the angular position of the rotor flux) and applies the digital low-pass filter to the estimated speed in order to calculate the equivalent motor speed.

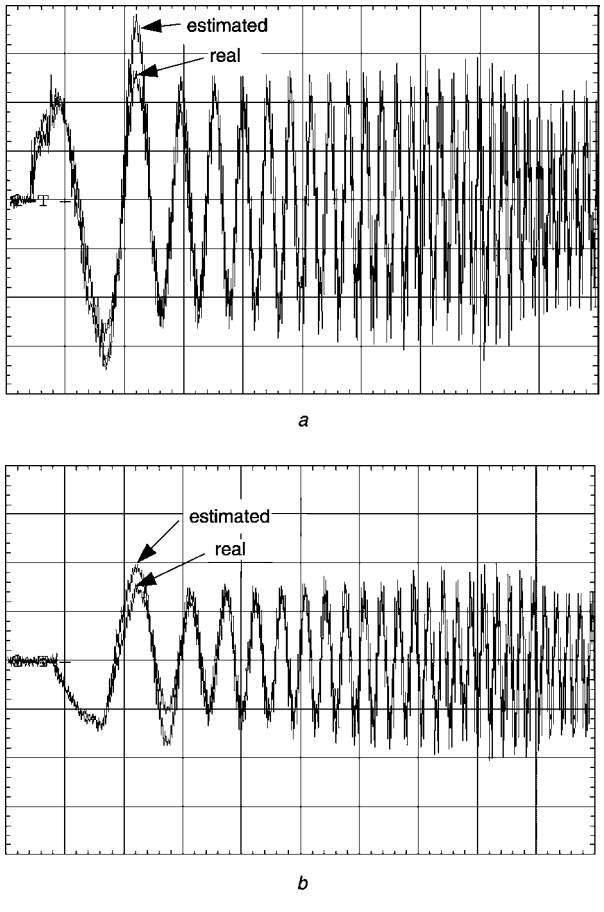

Fig. 3

a i_{qs} and $\hat{i}_{qs}$ with soft start within 0.8 s (no load) CH1 and CH2 - 2.5 A/division
b i_{qs} and $\hat{i}_{qs}$ with soft start within 0.8 s (full load) CH1 and CH2 - 6 A/division

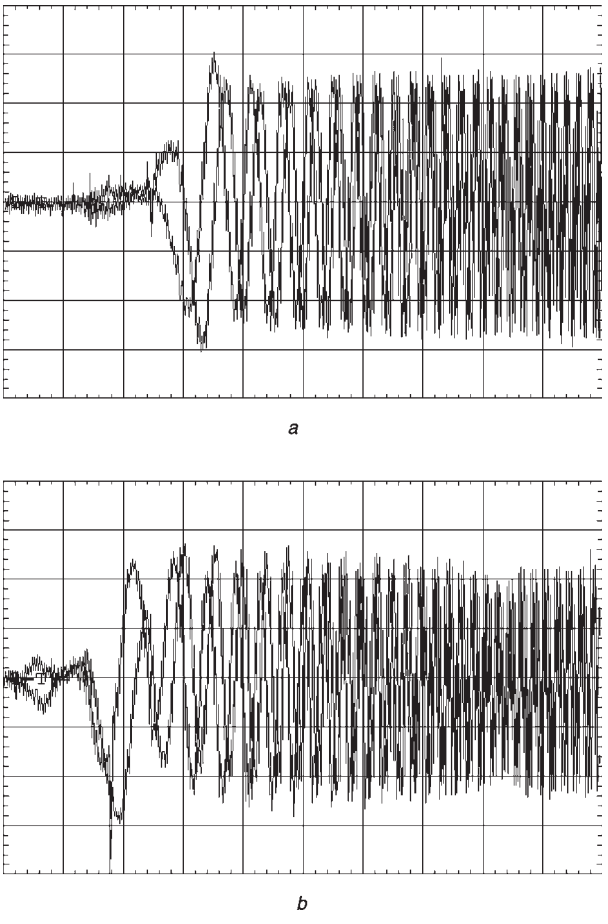

Fig. 4

a $\hat{\lambda}_{qr}$ and $\hat{\lambda}_{dr}$ with soft start within 0.8 s (no load)
b $\hat{\lambda}_{qr}$ and $\hat{\lambda}_{dr}$ with soft start within 0.8 s (full load)

4.2 Experimental Results

Appendix D presents the motor characteristics that were used in the implemental setup.

Figures 3*a* and 3*b* show the measurement current component i_{qs} and the estimated $\hat{i}_{qs}$ during soft start within 0.8 s. with no load and full load respectively.

Both Figures show that the proposed sensorless observer estimates the real current without significant error above 4 Hz. Below 4 Hz there is a small error which can be minimised, as previously explained, using variable speed gain.

Figures 4*a* and 4*b* show the estimated rotor flux during soft start within 0.8 s with no load and full load respectively.

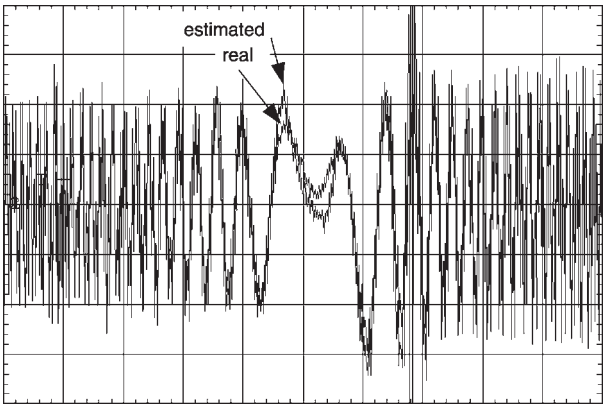

Fig. 5 *i_{qs} and $\hat{i}_{qs}$ in forward to reverse operation (no load) with a 0.8 s acceleration and a 0.8 s deceleration*

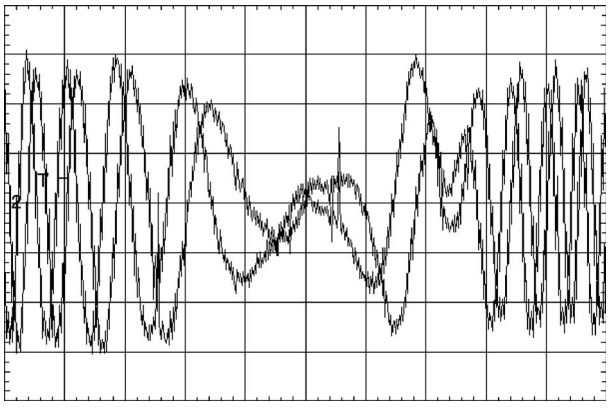

Fig. 6 *$\hat{\lambda}_{qr}$ and $\hat{\lambda}_{dr}$ in forward to reverse operation (no load) with a 0.8 s acceleration and 0.8 s deceleration*

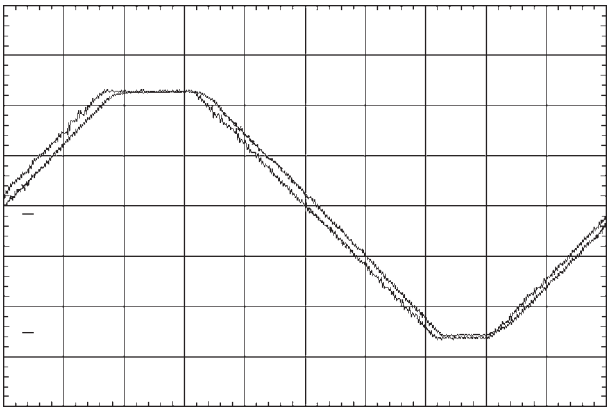

Fig. 8 *Speed estimation using digital low-pass filter. Forward to reverse operation*

Figures 5 and 6 show the transient response of the proposed observer during forward to reverse operation. As can be seen from Figs. 5 and 6, the proposed sensorless observer exhibits a robust operation without using a PI controller whose convergence depends on the frequency.

Figures 7*a* and 7*b* show the estimated flux during steady-state operation at 50 and 5 Hz respectively. These waveforms show that the estimated flux is unaffected by a fast change in the estimated speed based on the sliding-mode technique.

Finally, Fig. 8 shows the speed estimation during the forward to reverse operation. As can be seen the equivalent estimated speed is equal to the real one during the steady-state operation. During transient operation the equivalent estimated speed has a small phase shift due to the low-pass filter.

Figures 9*a* and 9*b* show the response of the conventional method in the case of uncorrected PI gains. The following equation shows the feedback of the conventional method [10].

$$\hat{\omega}_r = K_{\mathrm{p}}\left(\bar{i}_{qs}\hat{\lambda}_{dr} - \bar{i}_{ds}\hat{\lambda}_{qr}\right) + \mathrm{K}_i \int \left(\bar{i}_{qs}\hat{\lambda}_{dr} - \bar{i}_{ds}\hat{\lambda}_{qr}\right) dt \tag{24}$$

It is obvious that the convergence of the system is directly dependent on the PI gains and the load. In order to see the

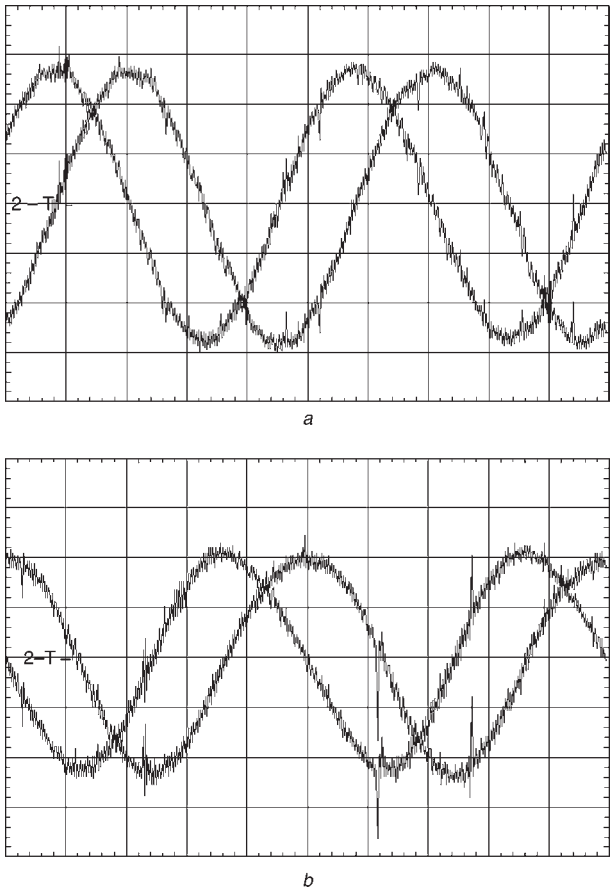

Fig. 7
a $\hat{\lambda}_{qr}$ and $\hat{\lambda}_{dr}$ at 50 Hz, 1497 rpm (no load)
b $\hat{\lambda}_{qr}$ and $\hat{\lambda}_{dr}$ at 5 Hz, 135 rpm (no load)

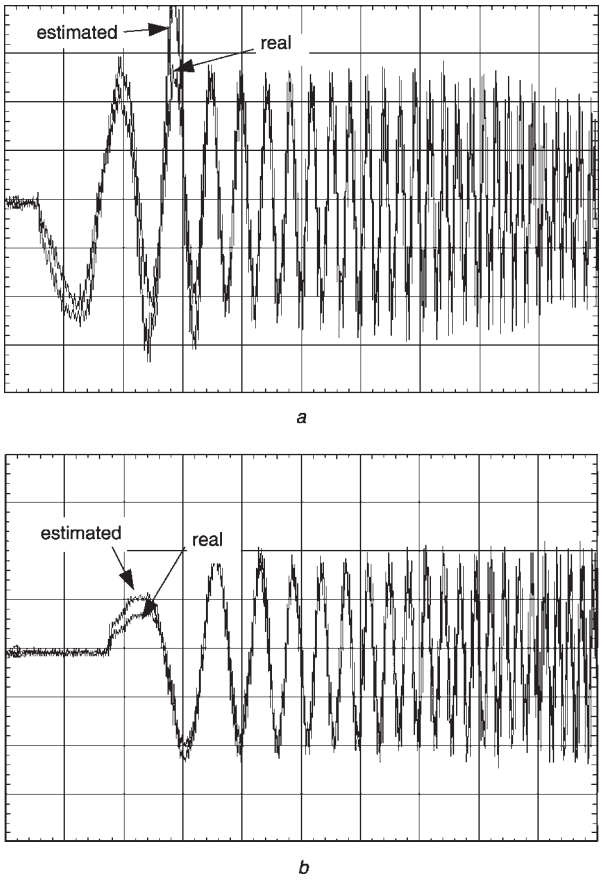

Fig. 9
a i_{qs} and $\hat{i}_{qs}$ with soft start within 0.8 s (no load) using uncorrected PI gains
b i_{qs} and $\hat{i}_{qs}$ with soft start within 0.8 s (full load) using uncorrected PI gains

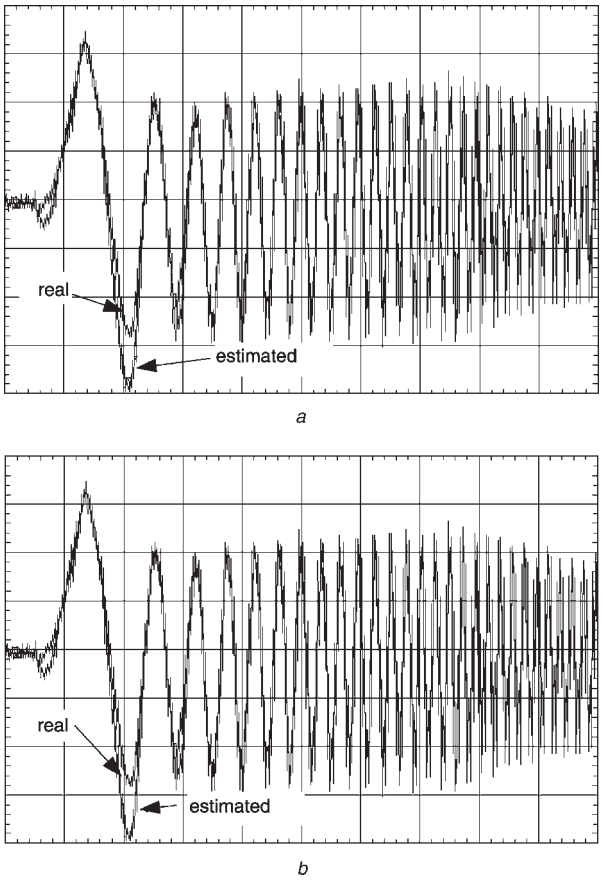

Fig. 10

a i_{qs} and $\hat{i}_{qs}$ with soft start within 0.8 s (no load) using uncorrected PI gains and sliding

b i_{qs} and $\hat{i}_{qs}$ with soft start within 0.8 s (full load) using uncorrected PI gains and sliding

advantages of the sliding-mode technique a combination of a PI controller and the sliding-mode technique has been tested using the following equation as feedback.

$$\hat{\omega}_{\mathrm{r}} = K_{\mathrm{p}}(\bar{i}_{qs}\hat{\lambda}_{dr} - \bar{i}_{ds}\hat{\lambda}_{qr}) + \mathrm{K_i}\int(\bar{i}_{qs}\hat{\lambda}_{dr} - \bar{i}_{ds}\hat{\lambda}_{qr})dt + K\mathrm{sgn}(\bar{i}_{qs}\hat{\lambda}_{dr} - \bar{i}_{ds}\hat{\lambda}_{qr}) \quad (25)$$

Figures 10*a* and 10*b* show the response of the system during the soft start using (25). Because of the sliding the systems follows the real value of the current (q-component) faster.

5 Conclusions

A sliding-mode observer for speed-sensorless induction motor drives has been presented. The purpose of the proposed observer is to estimate all the necessary values for direct torque vector control with robustness and efficiency. Its performance and behaviour has been analysed and tested using one of the most popular DSP controllers, the TMS320F240. Also, an analysis for the one and only observer gain has been made. Finally, experimental results confirm the robustness of the proposed observer to the parameter variation and its convergence without using a PI controller. Experimental results have shown the advantages of the proposed observer over a conventional method that uses a PI controller.

6 References

1 Vas, P.: 'Sensorless Vector and Direct Torque Control' (Oxford Univ. Press, Oxford, UK, 1998)
2 Atkinson, D.J., Acarnley, P.P., and Finch, J.W.: 'Observer for Induction Motor State Parameter Estimation', *IEEE Trans. Ind. Appl.*, 1991, **27**, (6)
3 Verghese, G.C., and Sanders, S.R.: 'Observers for Flux Estimation in Induction Machines', *IEEE Trans. Ind. Electron.*, 1988, **35**, (1)
4 Atkinson, D.J., Acarnley, P.P., and Finch, J.W.: 'Observers for Induction Motor State and Parameter Estimation', *IEEE Trans. Ind. Appl.*, 1991, **27**, (6), pp. 1119–1127
5 Schroedl, M.: 'Sensorless control of AC machines at low speed and standstill based on the 'INFORM' method', *Proc. IEEE-IAS Annual meeting*, 1996, **1**, pp. 270–277
6 Jansen, P.L., and Lorentz, R.D.: 'Transducer-less position and velocity estimation in induction and salient AC Machines', *IEEE Trans. Ind. Appl.*, 1995, **31**, pp. 240–247
7 Schauder, C.: 'Adaptive Speed Identification for Vector Control without Rotational Transducers', *IEEE Trans. Ind. Appl.*, 1992, **28**, (5)
8 Peng, F.Z., and Fukao, T.: 'Robust Speed Identification for Speed-Sensorless Vector Control of Induction Motors', *IEEE Trans. Ind. Appl.*, 1994, **30**, (5)
9 Maes, J., and Melkebeek, J.A.: 'Speed-Sensorless Direct Torque Control of Induction Motors Using an Adaptive Flux Observer', *IEEE Trans. Ind. Appl.*, 2000, **36**, (3)
10 Kubota, H., and Matsuse, K.: 'Speed Sensorless Field-Oriented Control of Induction Motor with Rotor Resistance Adaptation', *IEEE Trans. Ind. Appl.*, 1994, **30**, (5)
11 Hennenberg, G., Brunsbach, B.J., and Klepsch, T., 'Field oriented control of synchronous and asynchronous drives without mechanical sensors using Kalman filter'. Proc. European Conf. on Power electronics and applications (EPE), Florence, Italy, 1991, vol. 3, pp. 664–671
12 Kim, R., Sul, S.K., and Park, M.H.: 'Speed sensorless vector control of induction motor using extended Kalman filter', *IEEE Trans. Ind. Appl.*, 1994, **30**, pp. 1225–1233
13 Hurst, K.D., and Habetler, T.G.: 'Sensorless Speed Measurement Using Current Harmonic Spectral Estimation in Induction Machines Drives', *IEEE Trans Power Electron.*, 1996, **11**, (1)
14 Vas, P.: 'Artificial-Intelligence-Based Electrical Machines and Drives - Application of Fuzzy, Neural, Fuzzy-Neural and Genertic-Algorithm-Based Techniques' (Oxford Univ. Press, Oxford, UK, 1999)
15 Tursini, M., and Petrella, R.: 'Adaptive Sliding-Mode Observer for Speed-Sensorless Control of Induction Motors', *IEEE Trans. Ind. Appl.*, 2000, **36**, (5)
16 Kaletsanos, A., Xepapas, S.H., and Manias, S.N., 'A Novel Sliding Mode Fuzzy Logic Control Technique for Induction Motor Drive Systems'. Proc. Power electronics specialist Conf. (PESC), Vancouver, Canada, 17–21 June 2001, vol. 2, pp. 1209–1214
17 Utkin, V., Gulder, J., and Shi, J.: 'Sliding Mode Control in Electromechanical Systems' (Taylor & Francis, 1999)
18 Slotine, J.J., and Li, W.: 'Applied Non-linear Control' (Prentice Hall, 1991)

7 Appendices

7.1 Appendix A

The definition of the motor model constant values and the meaning of the symbols are the following:

$$n = \frac{R_{\mathrm{r}}}{L_{\mathrm{r}}},\ \sigma = 1 - \frac{L_{\mathrm{m}}^2}{L_{\mathrm{s}} \times L_{\mathrm{r}}},\ \beta = \frac{L_{\mathrm{m}}}{\sigma L_{\mathrm{s}} L_r},$$
$$\gamma = \frac{1}{\sigma L_{\mathrm{s}}}\left(R_{\mathrm{s}} + \frac{L_{\mathrm{m}}^2}{L_{\mathrm{r}}^2}R_{\mathrm{r}}\right)$$

where P is the number of poles, λ_{qr} and λ_{dr} are the rotor fluxes, J is the moment of inertia, i_{qs} and i_{ds} are the stator currents, L_{m} is the mutual inductance, T_{L} is the mechanical load, V_{qs} and V_{ds} are the stator voltages, ω_r is the motor rotational speed, $T_{\omega_{\mathrm{r}}}$ is the friction and airing loss, R_{s} and R_{r} are the stator-rotor resistances L_{s} and L_{r} are the stator-rotor self inductances, and T_{e} is the electromechanical torque.

7.2 Appendix B

The transfer function for the low-pass digital filter of the measured voltages and currents is the following:

$$H(z) = b(1) + b(2)z^{-1} + b(3)z^{-2} + \ldots + b(9)z^{-8}$$

where $b(1) = b(9) = 6.239\,78 \times 10^{-3}$, $b(2) = b(8) = 4.418\,73 \times 10^{-2}$, $b(3) = b(7) = 1.204\,17 \times 10^{-1}$ $b(4) = b(6) = 2.058\,12 \times 10^{-1}$, and $b(5) = 2.466\ 85 \times 10^{-1}$.

7.3 Appendix C: The discrete fourth-order Runge-Kutta method

Flux estimation: $y' = f(x, y, z), z' = g(x, y, z)$

$$y_{n+1} = y_n + \frac{1}{6}(k_1 + 2k_2 + 2k_3 + k_4)$$

$$z_{n+1} = z_n + \frac{1}{6}(l_1 + 2l_2 + 2l_3 + l_4)$$

$$k_1 = hf(x_n, y_n, z_n),\ l_1 = hg(x_n, y_n, z_n)$$

$$k_2 = hf\left(x_n + \frac{1}{2}h,\ y_n + \frac{1}{2}k_1,\ z_n + \frac{1}{2}l_1\right)$$

$$l_2 = hg\left(x_n + \frac{1}{2}h,\ y_n + \frac{1}{2}k_1,\ z_n + \frac{1}{2}l_1\right)$$

$$k_3 = hf\left(x_n + \frac{1}{2}h, y_n + \frac{1}{2}k_2,\ z_n + \frac{1}{2}l_2\right)$$

$$l_3 = hg\left(x_n + \frac{1}{2}h,\ y_n + \frac{1}{2}k_2,\ z_n + \frac{1}{2}l_2\right)$$

$$k_4 = hf(x_n + h,\ y_n + k_3,\ z_n + l_3)$$

$$l_4 = hg(x_n + h, y_n + k_3, z_n + l_3)$$

Current estimation: $y' = f(x, y)$

$$y_{n+1} = y_n + \frac{1}{6}(k_1 + 2k_2 + 2k_3 + k_4)$$

$$k_1 = hf(x_n, y_n)$$

$$k_2 = hf(x_n + \frac{1}{2}h,\ y_n + \frac{1}{2}k_1)$$

$$k_3 = hf(x_n + \frac{1}{2}h,\ y_n + \frac{1}{2}k_2)$$

$$k_4 = hf(x_n + h,\ y_n + k_3)$$

7.4 Appendix D: Motor model characteristics

Pole pairs:	2
Rated power:	1.5 kW
Rated voltage:	230 V rms
Rated current:	6,23 A rms
Rated torque:	10 Nm
Rated speed:	1490 rpm
R_s	2,5 Ω
R_r	2,5 Ω
L_s	0.0150 H
L_r	0.0093 H
L_m	0.1220 H